CHEMISTRY JOURNAL OF MOLDOVA. General, Industrial and Ecological Chemistry. 2021, 16(2), 91-101
ISSN (p) 1857-1727 ISSN (e) 2345-1688
http://cjm.asm.md
http://dx.doi.org/10.19261/cjm.2021.913

SYNTHETIC ZEOLITES MODIFIED WITH SALTS OF TRANSITION METALS IN THE REACTION OF CHEMISORPTION-CATALYTIC OXIDATION OF SULPHUR DIOXIDE BY AIR OXYGEN

Tatyana Rakitskaya, Tatyana Kiose*, Lyudmila Raskola

Faculty of Chemistry and Pharmacy, Odessa I.I. Mechnikov National University,
2, Dvoryanskaya str., Odessa 65082, Ukraine
**e-mail: kiosetatyana@gmail.com*

Abstract. The effect of the nature and concentration of *d*-metal salts attached to synthetic zeolites NaA and KA on the kinetic and stoichiometric parameters of the chemisorption-catalytic oxidation of sulphur dioxide with air oxygen at ambient temperature was studied. It was found that the adsorption capacity of NaA zeolite relative to SO_2 is 100 times higher than that of KA zeolite; the time of protective action of NaA and KA zeolites increases upon modification with transition metal salts and with an increase of their content in the compositions. It was shown that the formation of inner and outer sphere complexes and the relationship between them is determined by the nature and concentration of metal ions and by the nature of the carrier. It was proven that the chemisorption-catalytic process ends with the oxidation of SO_2 to H_2SO_4.

Keywords: sulphur dioxide, synthetic zeolite, oxidation, chemisorption-catalytic process, transition metal. photooxidation.

Received: 10 November 2021/ Revised final: 10 December 2021/ Accepted: 14 December 2021

Introduction

Sulphur dioxide is known as the most widespread environmental pollutant. Various chemisorbents and catalysts are commonly used to reduce its concentration in the air. The most effective chemisorbents are natural and synthetic zeolites [1-4], activated carbons [5], carbon fibre materials [6,7], metal oxides [1,8-10]. SO_2 is oxidized to H_2SO_4 at ambient temperature in the presence of dissolved metal complexes according to Eq.(1).

$$2SO_2 + O_2 + 2H_2O = 2H_2SO_4 \quad (1)$$

Numerous studies have been carried out on SO_2 oxidation in solutions and drops, which resulted in establishing the conditions of catalysis by compounds of Cu(II,III) [11,12], Fe(II,III) [13-16], Mn(II) [11,17 -19], Co(II) [20] and revealed the complexity of the kinetics and mechanisms of these reactions. Due to different conditions of research, in many cases there is a discrepancy between the results obtained by different authors. A generalizing analysis of the literature data [21-24] underlines the great importance for the theory of homogeneous catalytic oxidation reactions and for understanding the mechanisms of SO_2 conversion in the atmosphere. However, dissolved metal complex catalysts for SO_2 oxidation have limited application in air purification practice. Metal complex compounds fixed on various supports have numerous advantages, but the activity of such compositions has been studied scarcely in reactions with SO_2 [25-29]. The advantage of such catalysts is the simple technology of their preparation, the ability to vary their activity over a wide range due to the nature of the *d*-metal salts, the support, and other components that make up the catalyst compositions. Co^{2+}, Mn^{2+}, Cu^{2+}, Fe^{3+} and Pd^{2+} are used as metal ions of variable valence, and natural zeolites play the role of carriers [25-30]. Synthetic zeolites KA and NaA, CaA, NaX possess a high adsorption capacity in relation to SO_2 and provide protective properties for up to 120 minutes [3,4], however, these have not been practically studied as carriers of *d*-metal salts interacting with SO_2. Increasing the protective properties of synthetic zeolites in relation to SO_2 by modifying them with salts of transition metals is a question of current interest.

The aim of this work was set to study the effect of the nature and concentration of d-metals salts fixed on synthetic zeolites NaA and KA on the protective properties of compositions and stoichiometric parameters of sulphur dioxide chemisorption-catalytic oxidation by air oxygen at ambient temperature.

Experimental

Materials

$CuCl_2$, $Cu(NO_3)_2$, $CoCl_2$, $MnCl_2$, $NiCl_2$ (p.a. grade, Sigma-Aldrich, USA) and synthetic zeolites NaA and KA (Ishimbay specialized chemical plant of catalysts, Russia) were used in this study.

Methods

Synthetic zeolites NaA and KA with SiO_2/Al_2O_3= 2.0 were used in the work; the pH of the suspensions was 10.38 and 10.08, respectively. Samples of synthetic zeolites modified with salts of transition metals were obtained by the method of impregnation by moisture capacity: 10 g of zeolite NaA and KA zeolites dried at 110°C, with an average grain size of 0.75 mm were placed in a Petri dish, and then impregnated with aqueous solutions of salts MX_2 (M= Cu^{2+}, Co^{2+}, Mn^{2+}, Ni^{2+}; X= Cl^- , NO_3^-) (Sigma-Aldrich, USA) at given concentrations of components. Such choice of metal cations is due to their activity (excluding Ni^{2+}), in the reaction with SO_2 in the liquid phase [11,19,20]. The nature of the anion significantly affects the activity of transition metal cations in redox transformations [26,27]. The wet sample was dried in an oven in air at a temperature of 110°C to constant weight. The MX_2 content in the composition was calculated per unit weight of dry carrier.

Physical characterisation

X-ray phase analysis was carried out using a Siemens D500 (Germany) powder diffractometer in copper radiation (CuK_α, λ= 1.54178 Å), with a secondary beam graphite monochromator. To record the diffractograms, the test samples were thoroughly grinded in an agate mortar and placed in a glass cuvette with a working volume of 2×1×0.1 cm^3.

Scanning electron microscopy (SEM) studies of morphology and determination of local composition were performed by electron probe microanalysis on a scanning electron microscope JSM-6390LV (Japan).

Samples were examined by *IR spectroscopy* using Perkin Elmer FT-IR Spectrometer (USA) Frontier (400-4000 cm^{-1}, with a resolution of 4 cm^{-1}). The spectra were registered in KBr tablets obtained at a ratio of 1 mg of substance per 200 mg of KBr .

Thermogravimetric (DTG-DTA) investigation of initial and chemically modified synthetic zeolites samples (0.25 g) were performed on a Paulik F., Paulik D. and Erdey A. (Hungary) derivatograph with a four-channel microvolt recorder. The furnace temperature was increased at a heating rate of 10°C/min in the temperature range of 20-1000ºC with an accuracy of ±5%.

Investigation of the chemisorption-catalytic process

A gas-air mixture (GAM) with SO_2 concentration of 150 mg/m^3 was obtained by mixing a purified air flow and a flow of pure SO_2 in a special mixer. The initial and final concentrations of SO_2 were measured using a 667EKh08 electrochemical gas analyser (made by "Analitprilad", Ukraine) with the minimal detectable SO_2 concentration of 2 mg/m^3.

The dynamics of SO_2 adsorption onto the studied compositions was investigated in a flow-through gas thermostated at 20°C setup, in a glass reactor with a fixed layer of sorbent sample weighing 10 g under the following conditions: $C^{in}_{SO_2}$= 150 mg/m^3; t= 20°C; volumetric flow rate of GAM - 1 L/min, sorbent grain size of 0.5-1.0 mm, linear flow rate of GAM at 4.2 cm/s, relative humidity of GAM at 76%.

The amount of absorbed SO_2 (Q_{exp}, mol) was calculated using experimental data, which are given in the coordinates $\Delta C_{SO2} - \tau$. The stoichiometric parameter $n= Q_{exp}/Q_{theor}$ was calculated taking into account the stoichiometry of the reactions according to Eqs.(2,3).

$$SO_2 + 2Cu^{2+} + 2H_2O = H_2SO_4 + 2Cu^{+} + 2H^{+} \quad (2)$$

$$2SO_3^{2-} + M^{2+} = [M(SO_3)_2]^{2-} \quad (3)$$

where, M= Mn^{2+}, Co^{2+}, Ni^{2+}.

To assess the protective properties of synthetic zeolites and their modified metal salts forms, the following parameters were used: τ_0- period of time during which the dynamic absorption curve $C^f_{SO_2}$ = 0; τ_{GAM}- time of protective action; time to reach the maximum allowable concentration, for the working area it is 10 mg/m^3 [28].

Results and discussion

X-ray phase analysis of the studied zeolites

Diffraction patterns of the initial and modified with copper (II) chloride NaA and KA zeolites are shown in Figure 1(*a*)-(*d*) these are characterized by a set of reflections, the position and intensity of which correspond to the NaA and KA zeolites [31]. Additional reflections were not detected on the diffraction patterns of $CuCl_2/\bar{S}$ ($\bar{S}$ = NaA, KA) samples, the structure of zeolites did not undergo any changes, the interplanar distances did not change, but the intensity of the

base lines slightly decreased, which indicates on a decrease in the relative crystallinity (I_R, %) (Table 1). The crystallite sizes of the studied samples were calculated using Scherer's formula. As can be seen from the obtained results (Table 1), the crystallite sizes of the initial NaA and KA differ slightly, but are in accordance with the data [32]. The crystallite sizes decrease with the modification by copper(II) chloride, which indicates the amorphization of the samples.

Morphology of the zeolites

SEM images of NaA and KA samples and modified samples $CuCl_2/\overline{S}$ ($\overline{S}$ = NaA, KA) are presented in Figure 2. The following features are established. Characteristic depressions (cavities) filled with a fine-crystalline phase are found on the surface of the NaA zeolite (Figure 2*(a)*); clearly faceted cubic particles have a size of 0.7-1 μm. SEM images of the $CuCl_2$/NaA sample (Figure 2*(b)*) showed that the general surface appearance is similar to the original zeolite, but along with cubic crystals, crystallites with a broken shape are visible, indicating amorphization of the sample and lower relative crystallinity (Table 1). The surface morphology of the zeolite KA (Figure 2*(c)*) and the sample $CuCl_2$/KA (Figure 2*(d)*) differs from the above samples. There are no cavities on the surface of KA zeolite; aggregated particles have an irregular shape of cubes and spherulites (globules).

As can be seen from the data (Figure 2*(d)*), Cu(II) chloride does not make any noticeable changes in morphology. It should be noted that our data on the morphology of NaA zeolite are in agreement with the results [32]. There is no description of the morphology of KA zeolite in the available literature.

Table 1

X-ray spectral parameters of synthetic zeolites and their modified forms with $CuCl_2$.

Sample	*d, Å* (three reflections with the highest intensity)			I_R, %	*D, nm*
NaA	8.689	3.707	2.982	100	116.3
$CuCl_2$/NaA	8.686	3.706	2.981	92	103.2
KA	8.684	3.705	2.980	100	132.5
$CuCl_2$/KA	8.680	3.702	2.979	96	123.0

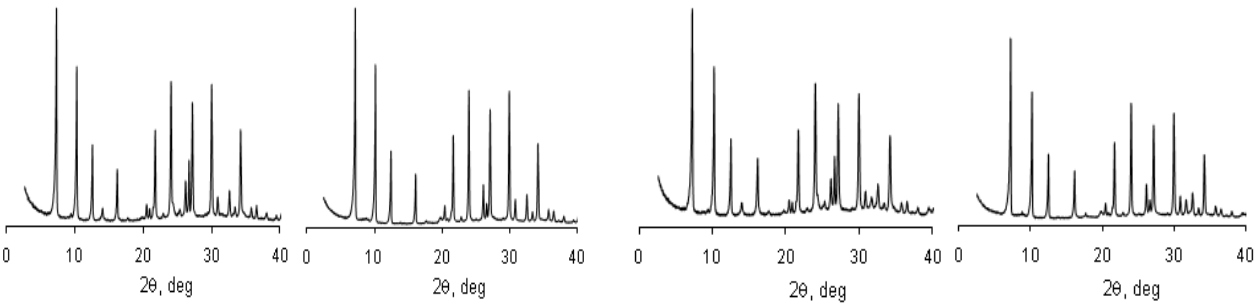

(a) ***(b)*** ***(c)*** ***(d)***

Figure 1. X-ray diffraction patterns of the initial samples of zeolites NaA (a), KA (b) and modified with $CuCl_2$ samples: $CuCl_2$/NaA (c); $CuCl_2$/KA (d).

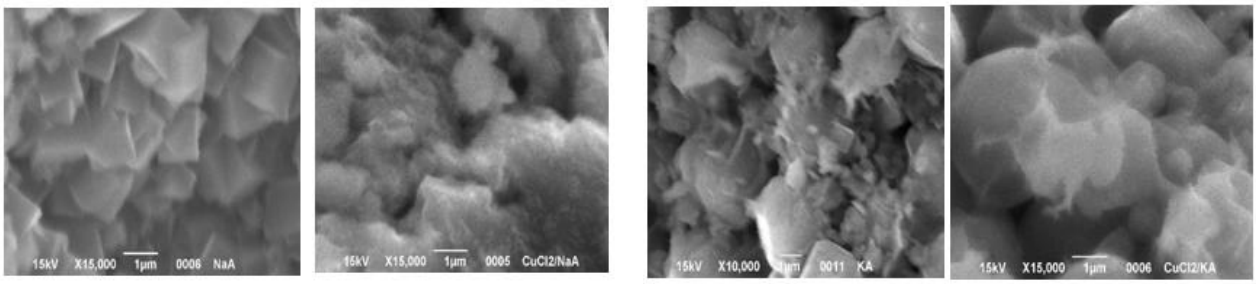

(a) ***(b)*** ***(c)*** ***(d)***

Figure 2. SEM images of samples NaA *(a)*, $CuCl_2$/NaA *(b)*, KA *(c)*, $CuCl_2$/KA *(d)*.

FT-IR investigations

Figure 3 shows a fragment of FT-IR spectra recorded for NaA and KA zeolites in the region of stretching and bending vibrations of the crystal framework. The bands were assigned according to the data from the literature [33]. The IR spectra of the two samples practically coincide and do not change upon the modification with metal salts. Adsorbed sulphur dioxide in the presence of air oxygen and water vapours on the surface of many carriers is converted into sulphuric acid [5-7].

Figure 3. FT-IR-spectra of samples KA *(1)* and NaA *(2)*.

The IR spectra of the initial NaA and KA samples, as well as after adsorption of SO_2, are almost identical. This is explained by the fact that the absorption bands of chemisorbed molecules of SO_2 and SO_4^{2-} ions [34–36], as well as absorption bands of synthetic zeolites, overlap.

For sulphate ion detection, NaA and KA samples were washed in distilled water, filtered off, and barium chloride solution was added to the filtrate; the formed precipitate was separated, washed and dried at 110°C. The IR spectra of the two precipitates show absorption bands for $BaSO_4$. In the case of NaA ν, cm^{-1}: 1196; 1117; 1078; 984; 609, and in the case of KA the absorption bands at 1192; 1125; 1083 cm^{-1} are less intense. The obtained data agree with the known values ν, cm^{-1}: 1199; 1108; 1072; 983; 609 from the literature [37].

Thermochemical properties

Figure 4 shows TG and DTG-DTA dehydration curves of NaA and KA zeolites samples and their forms modified with $CuCl_2$. Usually, dehydration of synthetic zeolites is accompanied by the loss of physically adsorbed water (≥100°C) and water molecules coordinated by cations (range from 100 to 350°C); dehydroxylation of surface groups occurs in the temperature range 320-540°C; isolated OH groups predominate at a temperature of >400°C [38,39].

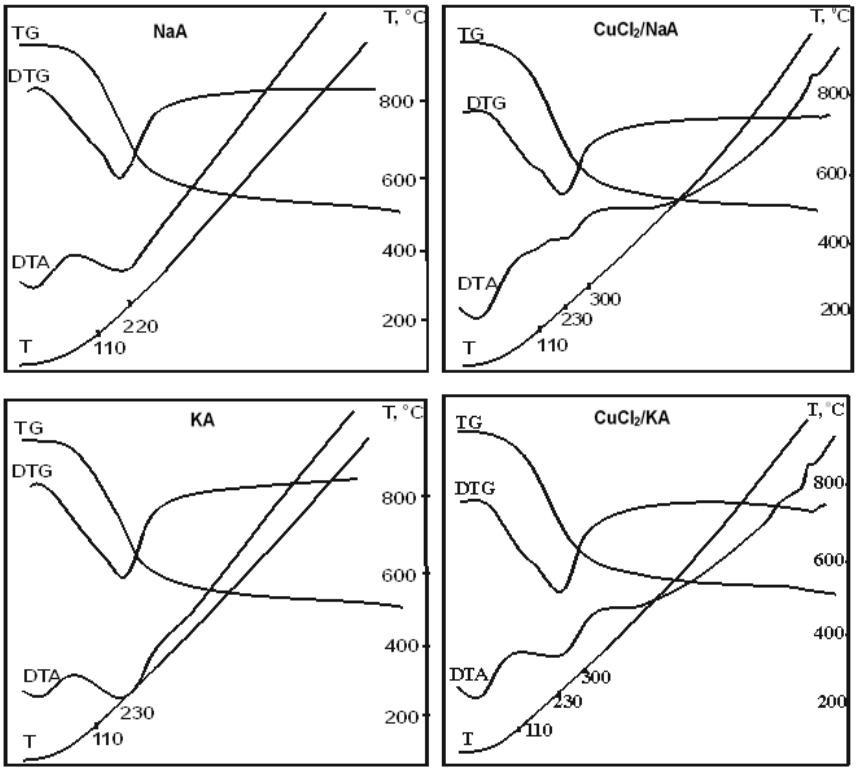

Figure 4. TGA curves of initial and modified with $CuCl_2$ chloride synthetic zeolites samples.

As can be noticed from the data of Figure 4 and Table 2, the initial NaA and KA zeolites have similar thermochemical characteristics, and the modification by copper(II) chloride leads to a decrease in the content of surface OH groups, which indicates the progress of the reaction according to Eq.(4), and Cu(II) is firmly held on the surface of the carrier as a result.

$$\begin{matrix}\text{T-OH}\\ \text{T-OH}\end{matrix} + CuCl_2 \leftrightarrow \begin{matrix}\text{T-O}\diagdown\\ \text{T-O}\diagup\end{matrix} Cu + 2HCl \qquad (4)$$

Kinetics of SO_2 adsorption by NaA and KA samples

The kinetics of SO_2 adsorption onto NaA and KA samples was studied. Figure 5 shows the time dependence of SO_2 final concentration ($C^f_{SO_2}$) after passing of the gas-air mixture through the adsorbent bed KA (curve 1) and NaA (curve 2). The kinetic curves have a characteristic form: the presence of areas where $C^f_{SO_2}$= 0; reaching the maximum permissible concentration for SO_2 after a certain time (τ_{max}) at the outlet of the reactor (MPC_{SO_2}= 10 mg/m^3); the adsorption process ends when $C^f_{SO_2} = C^{in}_{SO_2}$.

It can be seen that for the NaA zeolite the protective action time is 280 min, and for KA is only 3 min; zeolite NaA adsorbs $109 \cdot 10^{-5}$ mol of SO_2, which is 100 times more than for KA.

Hydrated NaA samples with different water content

It is known that the adsorption of water vapor suppresses the adsorption of SO_2 by various adsorbents [40]. Kinetic curves of SO_2 adsorption by hydrated NaA samples at different water content are shown in Figure 6. The profiles of the kinetic curves for air-dry (curve 1) and hydrated (curves 2-4) samples are similar, however, with an increase in m_{H_2O} the parameters τ_0, τ_{MPC} and Q_{exp} decrease.

Kinetics of adsorption of SO_2 by zeolites NaA, KA, modified with salts of transition metals

The influence of the nature of metal ions and anions, as well as the zeolite nature on the kinetics and mechanism of chemisorption-catalytic oxidation of SO_2 by air oxygen was studied on the samples $MX_2/\bar{S}$, where Cu^{2+}, Mn^{2+}, Co^{2+}, Ni^{2+}; X= Cl^-, NO_3^-; $\bar{S}$= NaA, KA.

Table 2

Results of thermogravimetric analysis of synthetic zeolites samples and forms modified with $CuCl_2$.

Sample	*T_M of endothermic effect, °C*	*Mass loss, %*				*C_{OH}, mmol/g*
		by T_M	*in the interval*			
			25-110°C	*25-300°C*	*25-1000°C*	
KA	230	9.6	2.0	13.6	18.8	5.8
NaA	220	9.2	2.4	13.6	18.8	5.8
$CuCl_2$/KA	230	9.6	2.0	13.6	18.0	4.9
$CuCl_2$/NaA	230	10.0	2.0	14.0	18.4	4.9

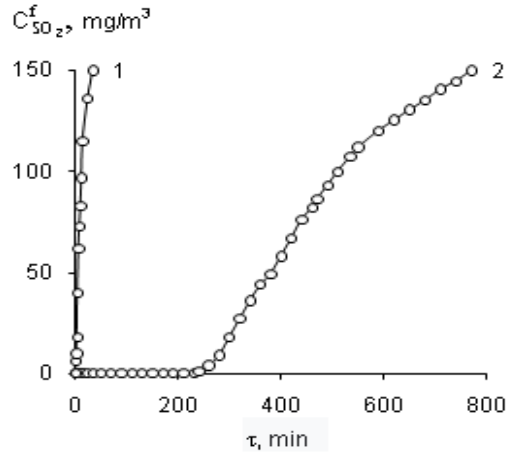

Figure 5. Time dependence of $C^f_{SO_2}$ for adsorption of SO_2 from gas-air mixture by air-dry zeolites KA *(1)* and NaA *(2)*.

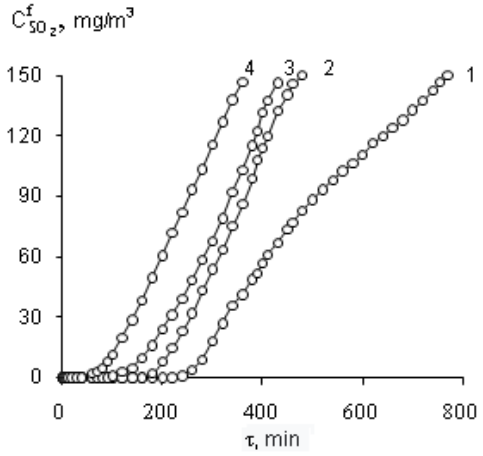

Figure 6. Time dependence of $C^f_{SO_2}$ for adsorption of SO_2 from the gas-air mixture at different water content on the NaA zeolite. m_{H_2O}, g/g: dry air *(1)*; 0.03 *(2)*; 0.06 *(3)*; 0.1 *(4)*

In the case of NaA zeolite, due to the high adsorption capacity and long protective action time, hydrated MX_2-H_2O/NaA samples (m_{H_2O} = 0.1 g/g) were used to determine the effect of MX_2 content on the kinetics of process. In the case of low-activity zeolite KA, air-dry MX_2/KA samples were used. Figure 7*(a)* and Figure 7*(b)* show the kinetic curves of $C^f_{SO_2}$ time dependence for samples CuX_2-H_2O/NaA and $CuCl_2$/ KA (Figure 7*(c)*). It can be noticed that, regardless of the Cu(II) precursor and the type of zeolite, the profiles of the kinetic curves are identical and are characterized by the parameters τ_0, τ_{MPC}. Based on the results of kinetic and stoichiometric data analysis (Table 3), the following conclusions can be drawn. With an increase in $C_{Cu(II)}$, regardless of the Cu(II) precursor, the parameters τ_0, τ_{MPC} and the amount of reacted sulphur dioxide (Q_{exp}) increase; the influence of the anion nature (Cl^-, NO_3^-) in the composition of the Cu(II) salt and the zeolite nature on the parameters of the SO_2 oxidation process is described by the following sequence: $CuCl_2$-H_2O/NaA> $Cu(NO_3)_2$-H_2O/NaA> $CuCl_2$ (KA). When determining the parameter *n*, the value of Q_{theor} was calculated taking into account the stoichiometry of reaction Eq.(1).

Thus, the obtained results show that in all cases, except for $C_{Cu(II)}$= $29\cdot10^{-5}$ mol/g, $Cu(NO_3)_2$-H_2O/NaA and $CuCl_2$/KA, Q_{exp}> Q_{theor}, which indicates multiple (*n*> 1) participation of Cu(II) in SO_2 oxidation by air oxygen.

Table 3

Effect of $C_{Cu(II)}$ on the protective and stoichiometric parameters of SO_2 oxidation by air oxygen in the presence of CuX_2/NaA(KA)-compositions.

$C_{Cu(II)}\cdot10^5$, mol/g	τ_0, min	τ_{MPC}, min	$Q_{exp}\cdot10^4$, mol SO_2	$Q_{theor}\cdot10^4$, mol SO_2 by (2)	*n*
$CuCl_2$-H_2O/NaA					
0	40	90	4.71	-	-
2.9	190	240	8.17	1.45	5.6
5.9	470	570	18.30	2.95	6.2
11.7	570	630	19.30	5.85	3.3
29.0	690	730	21.80	14.50	1.5
$Cu(NO_3)_2$-H_2O/NaA					
0	40	90	4.71	-	-
2.9	80	130	6.29	1.45	4.3
5.9	150	210	8.96	2.95	3.0
11.7	180	240	9.47	5.85	1.6
29.0	240	290	10.50	14.50	0.7
$CuCl_2$/KA					
0	1	3	0.17	-	-
2.9	80	130	4.06	1.45	2.8
5.9	110	145	6.09	2.95	2.1
11.7	150	180	7.00	5.85	1.2
29.0	200	250	7.56	14.50	0.5

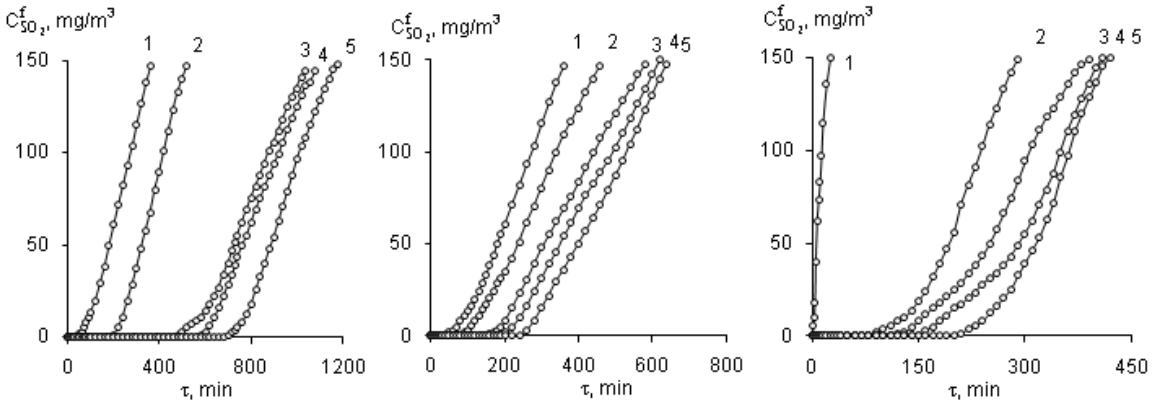

(a) ***(b)*** ***(c)***

Figure 7. Time dependence of $C^f_{SO_2}$ for SO_2 oxidation by air oxygen in the presence of $CuCl_2$-H_2O/NaA *(a)*, $Cu(NO_3)_2$-H_2O/NaA *(b)* and $CuCl_2$/KA *(c)* at different Cu(II) contents. $C_{Cu(II)}\cdot10^5$, mol/g: 0 *(1)*; 2-2.9 *(2)*; 5.9 *(3)*; 11.7 *(4)*; 29.0 *(5)*.

Figure 8 shows the typical kinetic curves for the oxidation of SO_2 by air oxygen in the presence of samples MCl_2-H_2O/NaA (Figure 8*(a)*) and MCl_2/KA (Figure 8*(b)*), where M= Mn^{2+}, Co^{2+}, Ni^{2+}; $C_{M(II)}$= $2.9\cdot10^{-5}$ mol/g. The profiles of the kinetic curves are identical and the parameters τ_0 and τ_{MPC} are determined by the nature of the metal ion and zeolite (Table 4). It should be noted that in the case of NaA, hydrated samples were studied, whereas in the case of KA air-dry samples were used. In this regard, only intra-series patterns can be considered. The following series of the influence of the nature of the metal ion on the time of the protective action of the samples were obtained: for hydrated NaA: Ni(II) < Co(II)< Mn(II); for air-dry KA: Ni(II)< Mn(II) < Co(II).

On the mechanism of surface complexes formation

The analysis of a large number of works showed that the immobilization of metal cations by zeolites is carried out by the mechanism of ion exchange and/or adsorption. According to the ion exchange mechanism, the ions present in the pores of the crystal lattice of zeolites (H^+, Na^+, K^+, Ca^{2+}, *etc.*) are replaced by metal ions from solutions. Chemisorption, which is an alternative mechanism of sorption, always leads to the formation of stable intra- and extraspheric complexes, where the functional groups of the zeolite framework form chemical bonds with metal ions [41]. Intraspheric complexes of transition metal ions are formed as a result of the following reactions according to Eqs.(5,6).

$$\equiv\text{T-OH} + M^{2+} \leftrightarrow \equiv \text{T-OM}^+ + H^+ \quad (5)$$

$$2\equiv\text{T-OH} + M^{2+} \leftrightarrow \equiv (\text{T-O})_2\text{M} + 2H^+ \quad (6)$$

The extraspheric complex is formed as a result of electrostatic interaction according with Eq.(7).

$$(\equiv\text{T-O}^-)_2 + M^{2+} \leftrightarrow (\equiv\text{T-O}^-)_2\text{---}M^{2+} \quad (7)$$

where, T is the symbol corresponding to the central atom of the surface, namely Si, Al.

Usually during the adsorption of metal ions, there are both intra- and extraspheric complexes, and their ratio can be determined by studying the desorption of metals.

Table 4

Protective and stoichiometric parameters of sulphur dioxide oxidation in the presence of compositions MCl_2/NaA(KA) by $C_{M(II)}$ = $2.9\cdot10^{-5}$ mol/g.

Sample	τ_0, *min*	τ_{MPC}, *min*	$Q_{exp}.10^4$ *mol* SO_2	$Q_{theor}\cdot10^4$, *mol* SO_2 *by (3)*	*n*
$NiCl_2$-H_2O/NaA	30	60	3.70	5.80	0.6
$MnCl_2$-H_2O/NaA	200	270	10.20	5.80	1.8
$CoCl_2$-H_2O/NaA	160	240	12.27	5.80	2.1
$NiCl_2$/KA	90	140	6.35	5.80	1.1
$MnCl_2$/KA	260	310	10.60	5.80	1.8
$CoCl_2$/KA	270	330	14.20	5.80	2.5

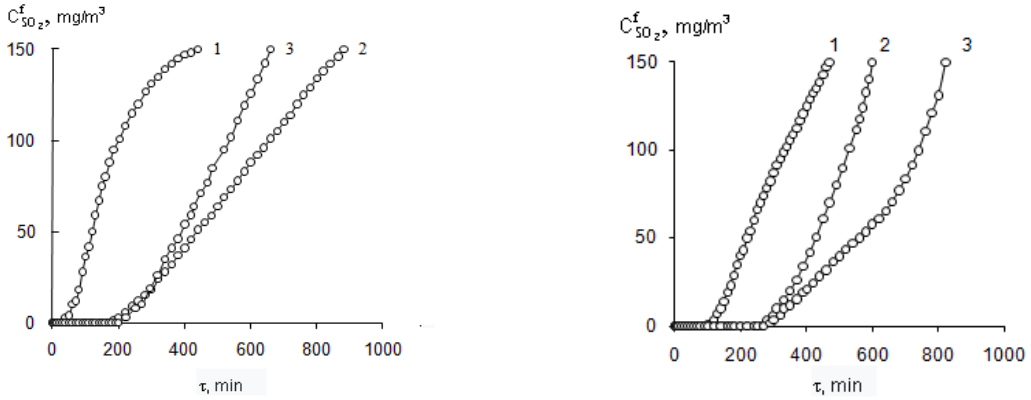

(a) ***(b)***

Figure 8. Time dependence of $C^f_{SO_2}$ for SO_2 oxidation by air oxygen in the presence of MCl_2/NaA *(a)* MCl_2/KA *(b)* compositions. M(II): Ni(II) *(1)*; Mn(II) *(2)*; Co(II) *(3)*.

Eq.(5) and Eq.(6) are supported by data on a decrease in the content of OH groups, for example, when Cu(II) chlorides are fixed on NaA and KA zeolites (Table 3). The formation of two types of surface complexes on the surface of zeolites was confirmed by experiments on desorption of metal ions with water at 20°C and by testing samples in a reaction with sulphur dioxide. Figure 9 shows the results of testing the initial $CuCl_2$-H_2O/NaA samples at the concentration $C_{Cu(II)}$= $2.9 \cdot 10^{-5}$ (curve 1) and $29.0 \cdot 10^{-5}$ mol/g (curve 2) and the same samples after desorption of Cu(II) ion (curves 4, 5), as well as the initial composition $CoCl_2$/KA at $C_{Co(II)}$= $2.9 \cdot 10^{-5}$ mol/g (curve 3) and after desorption of cobalt (II) (curve 6).

It can be seen that at $C_{Cu(II)}$= $2.9 \cdot 10^{-5}$ mol/g in the $CuCl_2$-H_2O/NaA sample, the profiles of the kinetic curves for the initial sample and after desorption in Cu (II) practically coincide (Figure 9*(a)*, curves 1, 4), which indicates the predominant formation of surface complexes by Eq.(5) or Eq.(6). With an increase in the content of copper (II) chloride to $29.0 \cdot 10^{-5}$ mol/g (Figure 9*(a)*, curve 2), two types of complexes are formed on the surface according to reactions 5-7. The outer-sphere copper (II) complex is easily desorbed by water, and the remaining copper (II) strongly bound to the surface ensures the oxidation of SO_2 (Figure 9*(a)*, curve 5). The data on testing the $CoCl_2$/KA sample before and after desorption of cobalt (II) (Figure 9*(b)*, curves 5,6) indicate that at $C_{Co(II)}$= $2.9 \cdot 10^{-5}$ mol/g, on the surface of the KA zeolite intra- and outer-sphere complexes are formed, the contribution of which to the total process of SO_2 oxidation is approximately the same.

On the mechanism of SO_2 oxidation by air oxygen

Sulphur dioxide is a reducing agent for which the values of the redox potential depend on the pH of the medium. For suspensions of synthetic zeolites NaA and KA, the pH of the suspension is in the range of 10.08-10.38, so the most possible will be the following electrochemical reaction according to Eq.(8).

$$SO_4^{2-} + H_2O + 2e = SO_3^{2-} + 2OH^- \quad (-0.93\ V) \qquad (8)$$

Due to the orbital mismatch, SO_2 and O_2 molecules do not react directly with each other by Eq.(1). In order to lift the symmetry ban, transition metal ions are used [42], the mechanisms of action of which have been studied in detail for homogeneous liquid-phase reactions and are generalized in [21-24,41]. The literature discusses mainly three types of mechanisms: radical-chain with one electron transfer [13,16, 21-23], non-radical with two electrons [18,19] and combined, which includes elements of the two previous mechanisms [16]. In the case of a radical mechanism, the first stage of the chain initiation in general will be written as follows, according to Eq.(9).

$$M^{n+} + SO_3^{2-} \rightarrow SO_3^{\bullet -} + M^{(n-1)+} \qquad (9)$$

This reaction most often occurs when M^{n+}= Cu^{2+} [11], Fe^{3+} [11,15,16]. Next, oxygen interacts with the sulphite radical according to Eq.(10).

$$SO_3^{\bullet -} + O_2 \rightarrow SO_5^{\bullet -} \qquad (10)$$

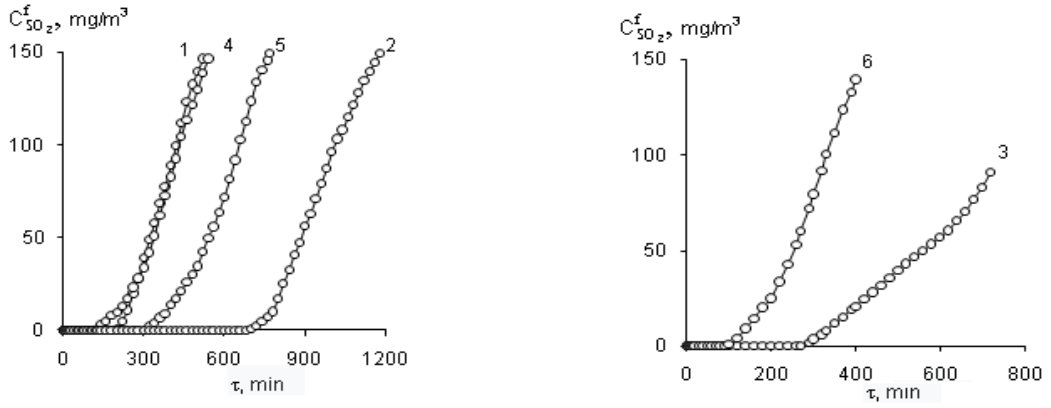

(a) ***(b)***

Figure 9. Time dependence of $C^f_{SO_2}$ for SO_2 oxidation by air oxygen with initial compositions $CuCl_2$-H_2O/NaA *(1,2) (a)* and $CoCl_2$/KA *(3) (b)* and with compositions after desorption of Cu (II) *(4,5) (a)* and Co (II) *(6) (b)* $C_{Cu(II)} \cdot 10^5$, mol/g: 2.9 *(1)*; 29.0 *(2)*; $C_{Co(II)} \cdot 10^5$, mol/g: 2.9 *(3)*.

The cycle ends with the return of M^{n+} in the reaction. There is evidence that the radical-chain mechanism is slowing down of the process through inhibitors, such as mannitol, which capture free radicals [43]. The general reaction scheme Eq.(1) in the presence of a $CuCl_2$ catalyst can be written as follows, according to Eqs.(11,12).

$$2CuCl_2 + SO_2 + 2H_2O = 2CuCl + H_2SO_4 + 2HCl, \quad (11)$$

$$4CuCl + O_2 + 4H^+ + 4Cl^- = 4CuCl_2 + 2H_2O. \quad (12)$$

According to Eq.(11), Cu(II) is reduced to Cu(I), and SO_2 is oxidized to sulphuric acid. Oxygen by Eq.(12) regenerates Cu(II) and returns it to the reaction; stoichiometric coefficient n> 1 (Table 4).

In the case of Co(II), Mn(II) and Ni(II), the interaction with SO_2 is more complicated, as corresponding ions have reduced form and are not able to take part in the reaction of chain initiation Eq.(9). In general, the most probable is a non-radical two-electronic mechanism, which is responsible for the internal spherical reaction according with Eq.(13-16) [17-19].

$$M^{2+} + SO_3^{2-} \leftrightarrow MSO_3 \quad (13)$$

$$MSO_3 + SO_3^{2-} \leftrightarrow [M(SO_3)_2]^{2-} \quad (14)$$

$$[M(SO_3)_2]^{2-} + O_2 \leftrightarrow [M(SO_3)_2 \cdot O_2]^{2-} \quad (15)$$

$$[M(SO_3)_2 \cdot O_2]^{2-} \leftrightarrow 2SO_4^{2-} + M^{2+} \quad (16)$$

As a result of the intermediate complex transformation, where the oxygen molecule interacts with coordinated sulphite ions, M^{2+} returns to the reaction cycle. In this case, the stoichiometric coefficient n must be determined taking into account the total Eq.(3). In the case of Mn(II), Co(II) and Ni(II) the mechanism of oxidation of these ions by oxygen to Mn(III), Co(III) and Ni(III) is not excluded, which occur very slowly in aqueous solutions [12,18]. In the case of fixation of Mn(II) and Co(II) on carriers due to the activation of the oxygen molecule by the surface [44], this process becomes more probable.

Conclusions

In the work, commercial synthetic zeolites of NaA and KA brands were used as carriers of transition metal salts. Chemisorption-catalytic compositions $MX_2/\bar{S}$ ($\bar{S}$= NaA, KA; M^{2+}= Cu, Mn, Co, Ni; X= Cl^-, NO_3^-) for the oxidation of sulphur dioxide with air oxygen at ambient temperature and high humidity were obtained. The initial carriers and chemisorption-catalytic compositions were studied by XRD, SEM, FT-IR spectroscopy, TG, DTG-DTA. Zeolites NaA and KA have the same parameters of the crystal structure, which do not change when modified with transition metal salts. Under their influence, a slight decrease in the relative crystallinity was observed.

The study has shown that NaA and KA samples differ in morphology. Clearly faceted cubic particles with a size of 0.7-1.0 μm were observed for zeolite NaA. Zeolite KA is characterized by aggregated particles of irregular shape of cubes and spherulites. When applying salts of transition metals, the shape of these particles is slightly disturbed.

According to the data of thermogravimetric analysis, the Cu(II) ions practically do not affect the temperature of the first (and only) endothermic effect, however, they reduce the content of OH groups due to the reaction of surface complexation.

It has been proven that the oxidation of SO_2 with atmospheric oxygen in the presence of $MX_2/\bar{S}$ compositions is a chemisorption catalytic process with a different mechanism of action of transition metal cations. In the case of Cu(II), it is reduced with SO_2 to Cu(I), which is oxidized by atmospheric oxygen to Cu(II) and returns again to the reaction. In the case of Co(II), Mn(II), and Ni(II), the process proceeds through the formation of an intermediate complex with SO_2 and O_2 molecules and the inner-sphere oxidation of SO_2 to H_2SO_4.

References

1. Allen, S.J.; Ivanova, E.; Koumanova, B. Adsorption of sulfur dioxide on chemically modified natural clinoptilolite. Acid modification. Chemical Engineering Journal, 2009, 152(2-3), pp. 389-395. DOI: https://doi.org/10.1016/j.cej.2009.04.063
2. Mathieu, Y.; Tzanis, L.; Soulard, M.; Patarin, J.; Vierling, M.; Molière, M. Adsorption of SO_x by oxide materials: A review. Fuel *Processing Technology*, 2013, 144, pp. 81-100. DOI: https://doi.org/10.1016/j.fuproc.2013.03.019
3. Gupta, A.; Gaur, V.; Verma, N. Breakthrough analysis for adsorption of sulfur-dioxide over zeolites. Chemical Engineering and Processing: Process Intensification, 2004, 43(1), pp. 9-22. DOI: https://doi.org/10.1016/S0255-2701(02)00213-1
4. Liu, Y.; Bisson, T.M.; Yang, H.; Xu, Z. Recent developments in novel sorbets for flue gas clean up. Fuel *Processing Technology*, 2010, 91(10),

pp. 1175-1197.
DOI: https://doi.org/10.1016/j.fuproc.2010.04.015
5. Anurov, S.A. Physicochemical aspects of sulfur dioxide adsorption by carbon adsorbents. Russian Chemical Reviews, 1996, 65(8), pp. 718-732. (in Russian) DOI: https://doi.org/10.1070/RC1996v065n08ABEH000221
6. Martin, C.; Perrard, A.; Joly, J.P.; Gaillard, F.; Delecroix, V. Dynamic adsorption on activated carbons of SO_2 traces in air: I. Adsorption capacities. Carbon, 2002, 40(12), pp. 2235-2246. DOI: https://doi.org/10.1016/S0008-6223(02)00108-2
7. Gaur, V.; Asthana, R.; Verma, N. Removal of SO_2 by activated carbon fibers in the presence of O_2 and H_2O. Carbon, 2006, 44(1), pp. 46-60. DOI: https://doi.org/10.1016/j.carbon.2005.07.012
8. Long, J.W.; Wallace, J.M.; Peterson, G.W.; Huynh, K. Manganese oxide nanoarchitectures as broad-spectrum sorbents for toxic gases. *ACS Applied Materials & Interfaces*, 2016, 8(2), pp. 1184-1193. DOI: https://doi.org/10.1021/acsami.5b09508
9. Jia, Z.H.; Liu, Z.Y.; Zhao, Y.H. Kinetics of SO_2 removal from flue gas on CuO/Al_2O_3 sorbent-catalyst. *Chemical Engineering & Technology*, 2007, 30(9), pp. 1221-1227. DOI: https://doi.org/10.1002/ceat.200700139
10. Cheng, W.P.; Zhao, J.Z.; Yang, J.G. MgAlFeCu mixed oxides for SO_2 removal capacity: Influence of the copper and aluminum incorporation method. *Catalysis Communications*, 2012, 23, pp. 1-4. DOI: https://doi.org/10.1016/j.catcom.2012.02.024
11. Grgić, I.; Hudnik, V.; Bizjak, M.; Levec, J. Aqueous S(IV) oxidation – I. Catalytic effects of some metal ions. *Atmospheric Environment*, 1991, 25A(8), pp. 1591-1597. DOI: https://doi.org/10.1016/0960-1686(91)90017-2
12. Anast, J.M.; Margerum, D.W. Trivalent copper catalysis of the autoxidation of sulfite. Kinetics and mechanism of the copper(III/II) tetraglycine reactions with sulfite. *Inorganic Chemistry*, 1981, 20(7), pp. 2319-2326. DOI: https://doi.org/10.1021/ic50221a075
13. McElroy, W.J.; Waygood, S.J. Kinetics of the reactions of the SO_4^- radical with SO_4^-, $S_2O_8^{2-}$, H_2O and Fe^{2+}. Journal of the *Chemical Society, Faraday Transactions*, 1990, 86(14), pp. 2557-2564. DOI: https://doi.org/10.1039/FT9908602557
14. Sato, T.; Gotto, T.; Okabe, T.; Lawson, F. The oxidation of iron(II) sulfate with sulfur dioxide and oxygen mixtures. Bulletin of the *Chemical Society* of *Japan*, 1984, 57(8), pp. 2082-2086. DOI: https://doi.org/10.1246/bcsj.57.2082
15. Bal Reddy, K.; van Eldik, R. Kinetics and mechanism of the suifite-induced autoxidation of Fe(II) in acidic aqueous solution. *Atmospheric Environment*, 1992, 26A(4), pp. 661-665. DOI: https://doi.org/10.1016/0960-1686(92)90177-M
16. Brandt, C.; Fabian, I.; van Eldik, R. Kinetics and mechanism of the iron(III)-catalyzed autoxidation of sulfur(IV) oxides in aqueous solution. Evidence for the redox cycling of iron in the presence of oxygen and modeling of the overall reaction mechanism. Inorganic Chemistry, 1994, 33(4), pp. 687-701. DOI: https://doi.org/10.1021/ic00082a012
17. Ibusuki, T.; Barness, H.M. Manganese(II) catalyzed sulfur dioxide oxidation in aqueous solution at environmental concentrations. *Atmospheric Environment*, 1984, 18(1), pp. 145-151. DOI: https://doi.org/10.1016/0004-6981(84)90237-3
18. Siskos, P.A.; Peterson, N.C.; Huie, R.E. Kinetics of the manganese(III)-sulfur(IV) reaction in aqueous perchloric acid solutions. *Inorganic Chemistry*, 1984, 23(8), pp. 1134-1137. DOI: https://doi.org/10.1021/ic00176a024
19. Berglund, J.; Elding, L.I. Manganese-catalysed autoxidation of dissolved sulfur dioxide in the atmospheric aqueous phase. *Atmospheric Environment*, 1995, 29, pp. 1379-1391. DOI: https://doi.org/10.1016/1352-2310(95)91318-M
20. Coichev, N.; van Eldik, R. Kinetics and mechanism of the sulfite-induced autoxidation of cobalt(II) in aqueous azide medium. *Inorganic Chemistry*, 1991, 30(10), pp. 2375-2380. DOI: https://doi.org/10.1021/ic00010a028
21. Ermakov, A.N.; Purmal, A.P. Catalytic mechanism of the "noncatalytic autooxidation of sulfite. Kinetics and catalysis, 2001, 42(4), pp. 479-489. DOI: https://doi.org/10.1023/A:1010565304435
22. Ermakov, A.N.; Purmal, A.P. Catalysis of HSO_3^- /HSO_3^{2-} oxidation by manganese ions. Kinetics and catalysis, 2002, 43(2), pp. 249-260. DOI: https://doi.org/10.1023/A:1015328829974
23. Ermakov, A.N.; Larin, I.K.; Ugarov, A.A.; Purmal, A.P. Iron Catalysis of SO2 Oxidation in the Atmosphere. Kinetics and catalysis, 2003, 44(4), pp. 476-489. DOI: https://doi.org/10.1023/A:1025181715142
24. Golodov, V.A.; Kashnikova, L.V. Oxidation of sulfur dioxide in aqueous solutions. Russian Chemical Reviews, 1981, 57(11), pp. 1796-1814. (in Russian). DOI: https://doi.org/10.1070/RC1988v057n11ABEH003409
25. Ivanova, E.; Kuomanova, B. Adsorption of sulfur dioxide on natural clinoptilolite chemically modified with salt solutions. *Journal of Hazardous Materials*, 2009, 167(1-3), pp. 306-312. DOI: https://doi.org/10.1016/j.jhazmat.2008.12.124
26. Rakitskaya, T.L.; Kiose, T.A.; Golubchik, K.O.; Dzhiga, G.M.; Ennan, A.A.; Volkova, V.Y Catalytic compositions based on chlorides of d-metals and natural aluminosilicates for the low-temperature sulfur dioxide oxidation with air oxygen. Acta Physica Polonica A, 2018, 133, pp. 1074-1078. DOI: http://doi.org/10.12693/APhysPolA.133.1074
27. Rakitskaya, T.L.; Kameneva, E.V.; Kiose, T.A.; Volkova, V.Ya. Natural clinoptilolite based solid-state compositions for low-temperature air purification from sulphur dioxide. Solid State Phenomena, 2015, 230, pp. 291-296. DOI: https://doi.org/10.4028/www.scientific.net/SSP.230.291

28. Rakitskaya, T.L.; Kiose, T.A.; Raskola, L.A.; Golubchik, K.O.; Shulga, A.B.; Nazar, A.P.; Stoyan, A.A. Natural clinoptilolite anchored chlorides of 3d metals in the reaction of low-temperature sulfur dioxide oxidation with air oxygen. Odesa National University Herald. Chemistry, 2018, 23(2(66)), pp. 6-17. (in Ukrainian). DOI: https://doi.org/10.18524/2304-0947.2018.2(66).132035
29. Kiose, T.A.; Rakitskaya, T.L.; Nazar, A.P.; Raskola, L.A. Mono- and bimetallic compositions anchored on natural tripoli in the reaction of sulfur dioxide oxidation with air oxygen. Odesa National University Herald. Chemistry, 2019, 24(4(72)), pp. 6-17. (in Ukrainian). DOI: http://doi.org/10.18524/2304-0947.2019.4(72).185513
30. Kiose, T.A. The effect of sulfur dioxide adsorption on the catalytic activity of supported copper-palladium complexes in the reaction of low-temperature carbon monoxide oxidation with air oxygen. Odesa National University Herald. Chemistry, 2013, 18(1(45)), pp. 51-56. (in Ukrainian). DOI: https://doi.org/10.18524/2304-0947.2013.1(45).31679
31. Treacy, M.N.J.; Higgins, J.B. Collection of simulated XRD powder patterns for zeolites. Amsterdam: Elsevier, 2001, 586 p. https://www.elsevier.com/books/collection-of-simulated-xrd-powder-patterns-for-zeolites/treacy/978-0-444-50702-0
32. Gordina, N.E. Development of scientific foundations for the synthesis of sorbents based on zeolites and metal oxide systems for the purification of process gases and liquids. Ph.D. Thesis, Ivanovo State University of Chemistry and Technology, Russia, 2020. https://sciact.ihcp.ru/file/dissertation_file/101/download
33. Breck, D. Zeolite Molecular Sieves. Mir: Moscow, 1976, 778 p. (in Russian).
34. Stark, J.V.; Park, D.G.; Lagadic, I.; Klabunde, K.J. Nanoscale metal oxide particles / clusters as chemical reagents. Unique surface chemistry on magnesium oxide as shown by enhanced adsorption of acid gases (sulfur dioxide and carbon dioxide) and pressure dependence. *Chemistry* of Materials, 1996, 8(8), pp. 1904-1912. DOI: https://doi.org/10.1021/cm950583p
35. Datta, A.; Cavell, R.G.; Tower, R.W.; George, Z.M. Claus catalysis. 1. Adsorption of sulfur dioxide on the alumina catalyst studied by FTIR and EPR spectroscopy. *Journal of Physical Chemistry*, 1985, 89(3), pp. 443-449. DOI: https://doi.org/10.1021/j100249a014
36. Low, M.J.D.; Goodsel, A.J.; Takezawa, N. Reactions of gaseous pollutants with solids. I. Infrared study of the sorption of sulfur dioxide on calcium oxide. Environmental Science & Technology, 1971, 5(12), pp. 1191-1195. DOI: https://doi.org/10.1021/es60059a003
37. Nakamoto, K. IR and Raman spectra of inorganic and coordination compounds. Mir: Moscow, 1991, 536 p. (in Russian).
38. Rabo, J. Zeolite chemistry and catalysis. Mir: Moscow, 1980, 506 p. (in Russian).
39. Zhdanov, S.P.; Khvoshchev, S.S.; Samulevich, N.N. Synthetic zeolites. Moscow: Chimiya, 1981, 261 p. (in Russian).
40. Rakitskaya, T.L.; Kiose, T.A.; Kameneva, A.V. Adsorption properties of natural sorbents with respect to sulfur dioxide and water vapor. Himia, Fizika ta Tehnologia Poverhni, 2014, 5(1), pp. 56-63. (in Ukrainian). https://www.cpts.com.ua/index.php/cpts/article/view/262
41. Doula, M.K.; Ioannou, A. The effect of electrolyte anion on Cu adsorption-desorption by clinoptilolite. *Microporous* and *Mesoporous* Materials, 2003, 58(2), pp. 115-130. DOI: https://doi.org/10.1016/S1387-1811(02)00610-8
42. Dorfman, Ya.A. Liquid phase catalysis. Alma-Ata: Nauka of Kazakh SSR, 1981, 364 p. (in Russian).
43. Barron, C.H.; O'Hern, H.A. Reaction kinetics of sodium sulfite oxidation by the rapid-mixing method. *Chemical Engineering Science*, 1966, 21(5), pp. 397-404. DOI: https://doi.org/10.1016/0009-2509(66)85050-9
44. Lan, S.; Wang, X.; Xiang, Q.; Yin, H.; Tan, W.; Qiu, G.; Liu, F.; Zhang, J.; Feng, X. Mechanisms of Mn(II) catalytic oxidation on ferrihydrite surfaces and the formation of manganese (oxyhydr)oxides. Geochimica et Cosmochimica Acta, 2017, 211, pp. 79-96. DOI: https://doi.org/10.1016/j.gca.2017.04.044